Structures and Electronic Spectra of CdSe−Cys Complexes: Density Functional Theory Study of a Simple Peptide-Coated Nanocluster

Sang-Yoon Chung,[†] Sungyul Lee,*[,†] Christopher Liu,[‡] and Daniel Neuhauser*[,‡]

College of Environmental Science and Applied Chemistry (BK21), Kyunghee University, Kyungki-do 449-701, Korea, and Department of Chemistry and Biochemistry, University of California, Los Angeles, California 90095

Received: July 15, 2008; Revised Manuscript Received: September 28, 2008

We present density functional theory (DFT) structures and time-dependent DFT electronic excitation energies of several small CdSe nanoclusters with the composition Cd_nSe_n ($n = 3, 6, 10, 13$). We examine the effects on the geometries and excitation spectra of the nanoclusters induced by two chemical changes: peptide-binding and ligand passivation. We use cysteine (Cys) and cysteine-cysteine dipeptide (Cys−Cys) as model peptides and hydrogen atoms as surface-bound solvent ligands (or stabilizing agents). By comparing the results calculated for bare, hydrogen-passivated ($Cd_nSe_nH_{2n}$), as well as the corresponding Cys- and Cys−Cys- bound clusters (Cd_nSe_n−, $Cd_nSe_nH_{2n}$, −Cys, −Cys−Cys), we find that peptide-binding blue shifts the electronic excitations of bare nanoclusters, but red shifts those of hydrogen-passivated nanoclusters. The carboxyl oxygen and the sulfur atom tend to form a four-centered ring with adjacent two Cd atoms when the CdSe cluster forms covalent bonds with Cys or Cys−Cys. Further, this type of bonds may be distinguishable by significant red shifts of the excitation energies.

I. Introduction

Understanding and controlling the organic−inorganic interface offers new paradigms in materials science, engineering, chemistry, biology and medicine.[1] Bottom-up self-assembly of nanohybrids offers novel materials, electronics, and optical applications.[1−5] Nanocomposite materials could also be useful as biological probes for diagnosis and treatment of human diseases. Among the various candidates, peptide-coated II−VI semiconductor (ZnS/Se, CdS/Se/Te) nanocrystals possess appealing properties as fluorescent probes for biological imaging and detection.[6−10] CdSe particles and clusters[11−25] receive a lot of attention because their electronic and optical properties may be varied by controlling characteristics such as the size,[26−29] shape,[28,30] and composition.[31] It is well known that the absorption band gap in the CdSe cluster blue shifts with reduced size,[18] making them good quantum dots (QDs) photoemitting over a wide range of wavelengths. Ligand binding may produce significant changes in the optical properties of CdSe QDs; for example, there is a dramatic increase in photoluminescence quantum yield in CdSe particles with Se-rich surfaces, but not with Cd-rich surfaces.[31]

In addition to the useful intrinsic properties of CdSe nanoclusters, chemical functionalization proves very helpful in designing materials with specific electrical and the optical properties.[32−35] In particular, functionalization of inorganic clusters with biomolecules (or bioconjugation) is a direct route of conferring bioactivity to nanoclusters. One may fine-tune the binding selectivity of CdSe nanoclusters by combining with biomolecules such as polypeptides or DNA.[36,37] The diverse physicochemical properties of CdSe−biomolecule complexes have allowed their wide applications as fluorescent probes in biological imaging,[38−45] tunable absorbers and emitters in nanoscale electronics,[46] quantum dot lasers,[47] and biosensing.[32,48]

An increasing number of studies have attempted to understand the geometries, electronic, and optical properties of CdSe clusters in the context of ligand coordination[11−16] and composition stoichiometry.[49,50] CdSe clusters with organic ligands have been studied to determine the structures and optical properties as functions of the size and ligands. Ishikawa and co-workers[26] recently obtained the geometry of $(CdSe)_n$ clusters ($n \leq 13$) with stoichiometric composition[13−15] as the precursors nucleated in the solution phase synthesis of the large CdSe QDs by correlating their absorption, photoluminescence (PL), and X-ray diffraction (XRD) spectra with density functional theory (DFT) calculations. Peng and Peng[17] also studied the temporal shape evolution of CdSe quantum-confined nanorods (quantum rods) in nonaqueous solvents with organometallic precursors. Today, CdSe clusters conjugated with the organic or biochemical molecules are prominent examples of functionalized inorganic nanoclusters.

In the present work, we study a CdSe cluster−Cys and −Cys−Cys complex as a prototypical model for functionalized semiconductor clusters whose physicochemical properties may be fine-tuned by the effects of ligands. We model the biomolecule by using Cys and Cys−Cys due to its use as a bridging residue in peptide-coated nanoclusters. Our calculated results provide a bridge between the atomistic details of ligand complexation and the corresponding optical changes, giving insight into structural and optical changes attributable to biomolecule conjugation. The main interest experimentally is to see whether proteins will change the optical excitations.

While a refined DFT calculation of a semiconductor with a protein is quite challenging computationally, even a single amino acid with a cluster is important as it establishes the trend expected for larger system. Therefore, our results will contribute to an essential goal in chemistry: understanding of molecular structure (both geometrical and electronic) and its correlation

* To whom correspondence should be addressed. E-mail: (S.L.) sylee@khu.ac.kr; (D.N.) dxn@chem.ucla.edu.
[†] Kyunghee University.
[‡] University of California.

10.1021/jp8062299 CCC: $40.75
Published on Web 12/02/2008

with physical properties. In doing so, we bring hybrid nanostructures further into chemistry, following the tradition of applying molecular insights to build nanostructures. This study is therefore valuable for researchers who apply knowledge at the molecular level to the design of novel nanostructures.

We specifically obtain and compare results for the geometry, chemical bonding and the electronic spectra of Cd_nSe_n−Cys and −Cys−Cys (n = 3, 6, 10, 13) complexes. Since the $Cd_{13}Se_{13}$ cluster seems to be the smallest cluster exhibiting the structural features of the bulk CdSe[26] and is also amenable to the DFT and time-dependent DFT (TDDFT) methods employed in this work, we choose it to examine the trends in the structures and the electronic properties that may extrapolate to larger CdSe system as a function of bioconjugation and passivation. The overall motivation is a desire to bridge the optical properties of bioinorganic hybrids and an atomistic picture of the geometric structure and chemical bonding, and we examine the changes in these properties brought about by two chemical processes: biomolecule-binding and passivation. We study the effect of ligand passivation (such as solvents and stabilizing agents) by saturating the surface Cd and Se atoms with hydrogens ($Cd_nSe_nH_{2n}$). We predict that Cys- and Cys−Cys- binding blue shifts the electronic excitations of Cd_nSe_n bare nanoclusters, but red shifts those of hydrogen-passivated nanoclusters $Cd_nSe_nH_{2n}$. We also find that Cd−S (or both Cd−S and Cd−OOC) bond formation is characteristic of the CdSe−Cys (or CdSe−Cys−Cys system), which is distinguishable by a large (0.7∼1.4 eV) red shift of the excitation energies.

II. Computational Methods

We employ the DFT and TDDFT methods as implemented in Gaussian03.[51] Becke's three parameter hybrid method[52] and the correlation functional by Lee, Yang, and Parr[53] (B3LYP) are used with the 6-311++G** and the Lanl2dz basis set. Stationary structures are obtained by verifying that all the harmonic frequencies are real. Default options are employed for all optimizations. No symmetry constraints are imposed during the optimizations.

III. Results

The polynuclear inorganic complexes we study all involve an inorganic (CdSe) core. We refer to this inorganic part interchangeably as "nanocluster" or "core". We are interested in the effects of organic ligand (the amino acid Cys) complexation as well as hydrogen passivation. Hence we study the effects of Cys-binding alone, hydrogen passivation alone, or both together. As a result, there are four types of molecules studied here; first, the CdSe core possesses neither Cys nor surface ligands, and we describe them as "bare nanoclusters/cores". The core may be passivated by hydrogens but not bound to Cys, and we refer to these as "hydrogen-passivated nanoclusters". We also study the nanocluster that is Cys-bound but not hydrogen-passivated; we refer to these "Cys-bound nanoclusters". Last, hydrogen passivation and Cys-binding results in "hydrogen-passivated Cys-bound nanoclusters". The exact wording may differ slightly depending on context.

We first discuss the structures and electronic excitation of bare nanoclusters with composition (Cd_nSe_n, n = 3, 6, 10, 13). Then we compare them with their corresponding Cys-bound forms (Cd_nSe_n−Cys). Third, we will examine hydrogen passivation by comparing hydrogen-passivated nanoclusters with the bare counterparts. Finally, we examine the effects of Cys- and Cys−Cys- binding on hydrogen-passivated nanoclusters.

III-1. Validation of Computational Methodology. The nanoclusters studied in this article consist of coordinating organic molecules (C, N, O, S) and an inorganic core (Cd, Se). DFT is a well-tested computational method suitable for elements from various parts of the periodic table. However, certain exchange-correlation functionals are more accurate for inorganic elements, especially transition metals. To test the validity of our methodology, we briefly test the structures and electronic excitations of the Cd_nSe_n clusters on which experimental work exists. Figure 1 and Table 1 present the calculated structures, relative energies, and relative Gibbs free energies of the bare Cd_nSe_n (n = 3, 6, 10, 13) clusters.

III-2. Conformational Surface of Bare Nanoclusters. Here we discuss the symmetry and the relative stability of these structures. Overall, we find degenerate minima of different point group symmetries. In addition to the geometries reported by Ishikawa and co-workers[26] we find several higher-lying states on the conformation potential surface. Each Cd_nSe_n cluster exists in several different symmetry types of very similar energies. The lowest energy structure of the Cd_3Se_3 cluster is predicted to be of D_{3h}, but the isomer of C_{2v} symmetry is calculated to be higher only by 0.005 kcal/mol (0.7 kcal/mol in Gibbs free energy at 298 K), as given in the Supporting Information. Likewise, we find three lowest energy structures (C_i, C_1 and D_{3d}) of the Cd_6Se_6 cluster within 0.01 kcal/mol (1 kcal/mol in Gibbs free energy at 298 K). Therefore, we only discuss here the lowest energy structures.

We observe elongation of Cd−Se bonds in clusters of increasing sizes. We use the smallest cluster (n = 3) as reference. The Cd−Se bond length increases slightly from ∼2.6 Å for Cd_3Se_3 to ∼2.7 Å for $Cd_{10}Se_{10}$. Some Cd−Se bonds in $Cd_{10}Se_{10}$ are as long as 0.2 Å longer (∼2.8 Å) depending on the degree of saturation. We attribute this to differences in coordination environments as cluster size increases.

III-3. Conformational Surface of Cys-bound Bare Nanoclusters. In Figure 2, the calculated structures of the Cd_nSe_n−Cys (n = 3, 6, 10, 13) clusters are depicted, along with their relative energies and Gibbs free energies at 298 K. We find two isomers of Cd_3Se_3−Cys of similar energy, (3-c-1) and (3-c-2). The energies and Gibbs free energies (298 K) of the three Cd_6Se_6−Cys complexes, (6-c-1), (6-c-2), and (6-c-3) are also similar. The two $Cd_{10}Se_{10}$−Cys complexes have similar energies (within 1 kcal/mol), whereas the third lowest energy structure (10-c-3) lies somewhat higher (by ∼2 kcal/mol) in energy. However, the Gibbs free energy of (10-c-2) is lower than other two isomers, (10-c-1) and (10-c-3), by ∼1.5 kcal/mol. The same trend is seen for $Cd_{13}Se_{13}$. In all these low-energy structures of the Cd_nSe_n−Cys (n = 3, 6, 10, 13) complexes, the carbonyl oxygen atom of Cys strongly interacts with the Cd atom, whereas the amino group is located at the opposite side to the Cd−Se moiety. This result is in agreement with previous DFT studies.[54−56] Coordination of oxygen atoms to Cd atoms is similar to the coordination of phosphine oxide via the oxygen atom.[57−59] This is reasonable due to attraction between the oppositely charged cadmium and oxygen atoms. The carbonyl group is a dipole toward the oxygen atom. Cadmium atoms in CdSe nanoclusters are known to carry up to one full positive charge.[60]

III-4. Cys-Binding Blue Shifts the Excitation Energies of Bare Nanoclusters. Experimental advances have enabled synthesis of bare nanoclusters. TDDFT allows us to relate the geometries of our bare nanoclusters to their excitation energies. The electronic transition energies to the four lowest excited states of Cd_nSe_n clusters are given in Table 1 along with the

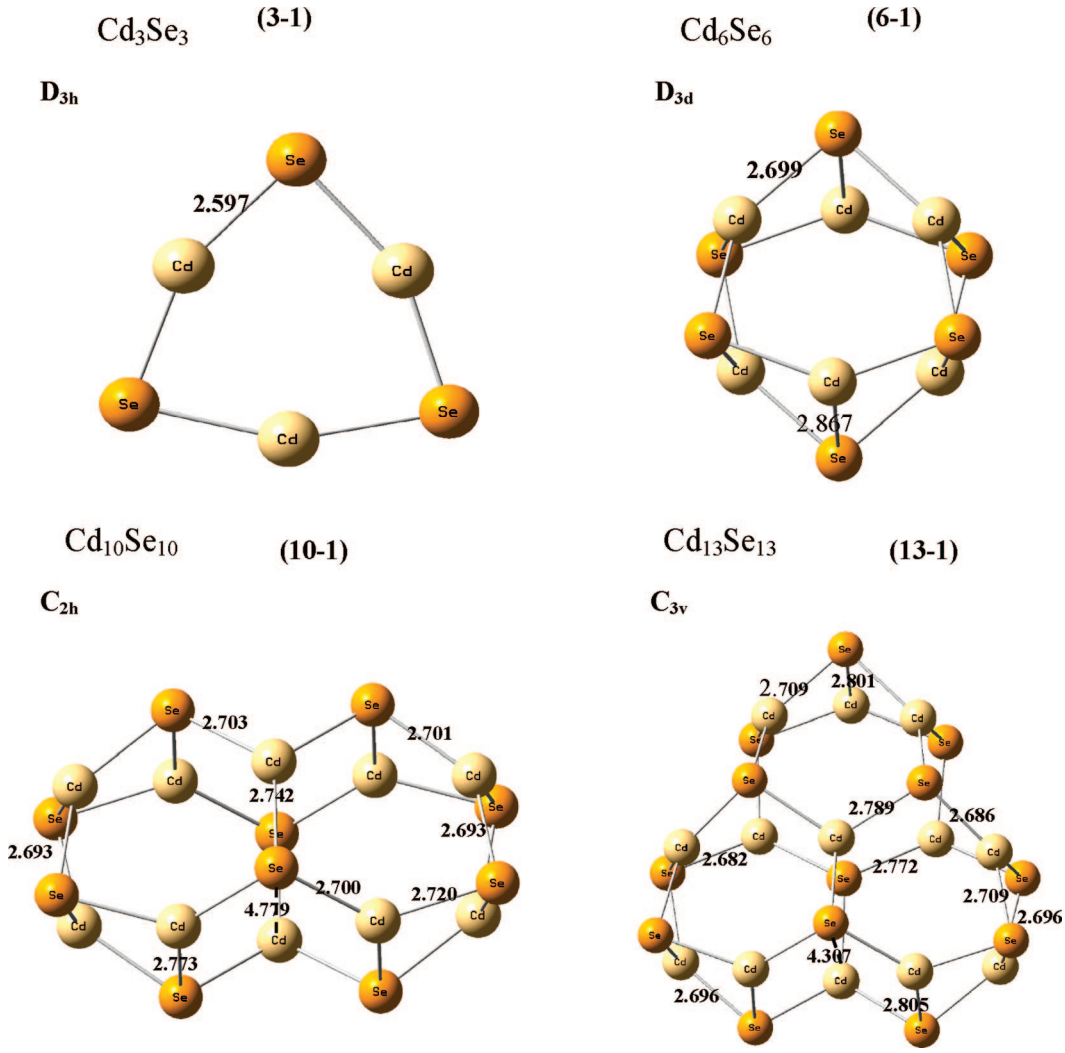

Figure 1. Geometry (bond lengths in Å) and point group of Cd_nSe_n (n = 3, 6, 10, 13).

TABLE 1: Electronic Energy *E* (Hartree), Zero Point Energy ZPE (kcal/mol), Vertical Electronic Excitation Energy VE (eV), and Oscillator Strength *f* to the Four Lowest Excited States of Bare Cd_nSe_n and Cd_nSe_n−Cys (n = 3, 6, 10, 13) Clusters

	E	ZPE	VE	*f*	symmetry
Cd_3Se_3					
(3−1)	−172.064535	2.3	2.44, 2.44, 2.87, 3.30	0.0000, 0.0000, 0.0392, 0.0000	$^1A'_1 \leftarrow X\ ^1A''_2$
Cd_3Se_3−Cys					
(3-c-1)	−894.163136	70.9	2.60, 2.68,3.05, 3.38	0.0001, 0.0008, 0.0450, 0.0133	
(3-c-2)	−894.162850	70.8	2.60, 2.65, 3.04, 3.37	0.0001, 0.0006, 0.0439, 0.0199	
Cd_6Se_6					
(6−1)	−344.222966	5.1	2.48, 2.48, 2.63, 2.94	0.0000, 0.0000, 0.0552, 0.0000	$^1A_g \leftarrow X\ ^1A_u$
Cd_6Se_6−Cys					
(6-c-1)	−1066.32153	73.8	2.57, 2.59, 2.73, 2.95	0.0007, 0.0009, 0.0606, 0.0066	
(6-c-2)	−1066.32137	73.7	2.57, 2.59,2.73, 2.94	0.0007, 0.0008, 0.0607, 0.0071	
(6-c-3)	−1066.32088	73.7	2.57, 2.58, 2.71, 2.93	0.0006, 0.0001, 0.0546, 0.0051	
$Cd_{10}Se_{10}$					
(10−1)	−573.762920	8.8	2.51, 2.64, 2.72, 2.72	0.0000, 0.0340, 0.0496, 0.0000	$^1A_g \leftarrow X\ ^1A_u$
$Cd_{10}Se_{10}$−Cys					
(10-c-1)	−1295.86323	77.7	2.60, 2.73, 2.75, 2.80	0.0004, 0.0330, 0.0079, 0.0390	
(10-c-2)	−1295.86233	77.4	2.53, 2.68,2.73, 2.79	0.0013, 0.0319, 0.0398, 0.0179	
(10-c-3)	−1295.86002	77.4	2.55, 2.69, 2.73, 2.76	0.0006, 0.0342, 0.0120, 0.0359	
$Cd_{13}Se_{13}$					
(13−1)	−745.922836	11.6	2.57, 2.57, 2.71, 2.80	0.0044, 0.0044, 0.0524, 0.0000	$^1A_1 \leftarrow X\ ^1A_1$
$Cd_{13}Se_{13}$−Cys					
(13-c-1)	−1468.02399	80.4	2.59, 2.62, 2.68, 2.80	0.0068, 0.0050, 0.0206, 0.0357	
(13-c-2)	−1468.02187	80.2	2.54, 2.61,2.73, 2.77	0.0048, 0.0057, 0.0490, 0.0166	
(13-c-3)	−1468.02000	80.2	2.61, 2.62, 2.72, 2.78	0.0046, 0.0054, 0.0318, 0.0299	

oscillator strengths. They are calculated to be 2.4−3.3 eV. The transition energies to the first excited states of Cd_nSe_n increase smoothly with cluster size (2.44, 2.48, 2.51, 2.57 eV for n = 3, 6, 10, 13). This can be understood by noting that the number

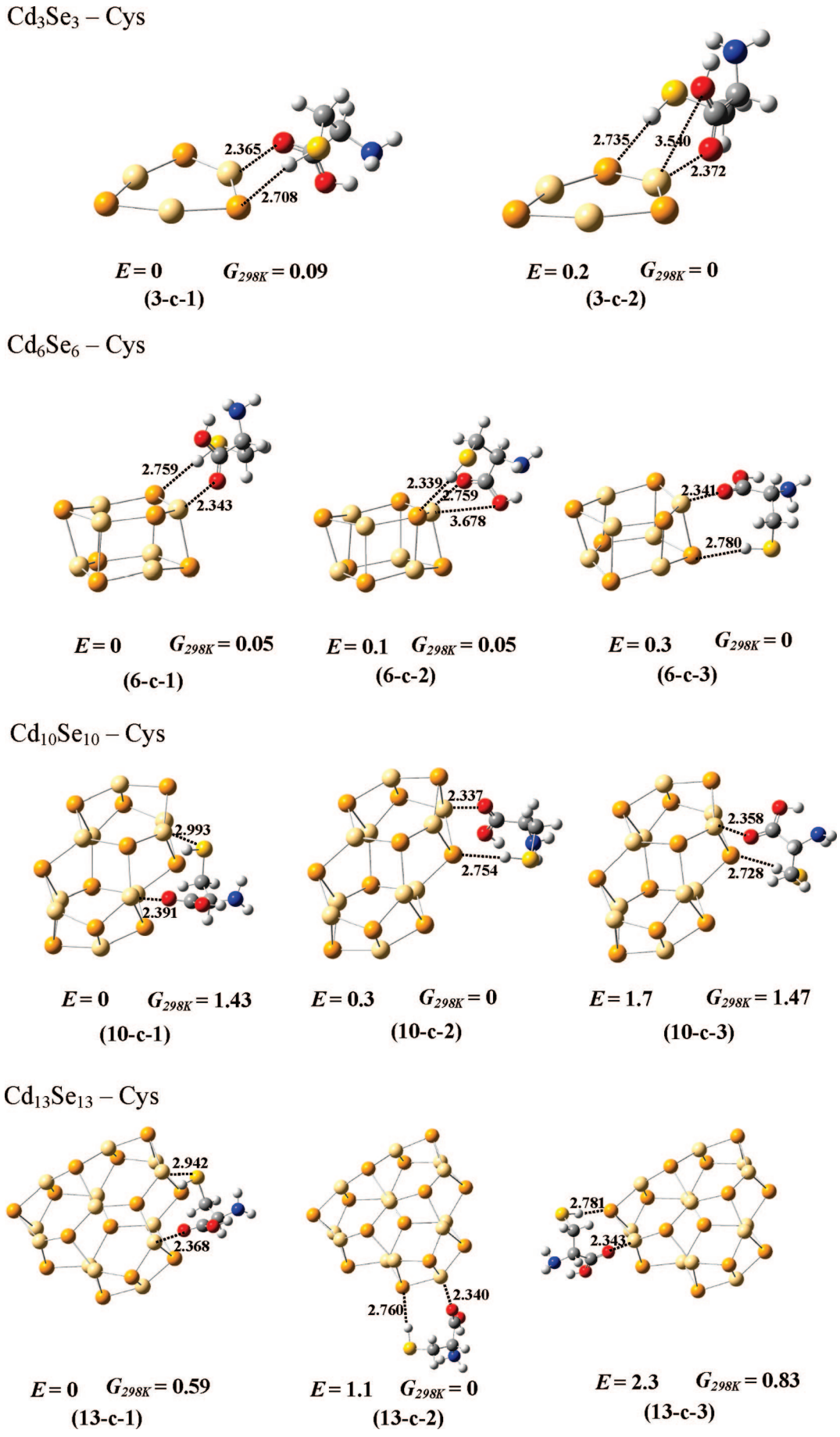

Figure 2. Geometry (bond lengths in Å) and relative energy (kcal/mol), and relative Gibbs free energy (kcal/mol, at 298 K) of Cd_nSe_n−Cys (n = 3, 6, 10, 13)

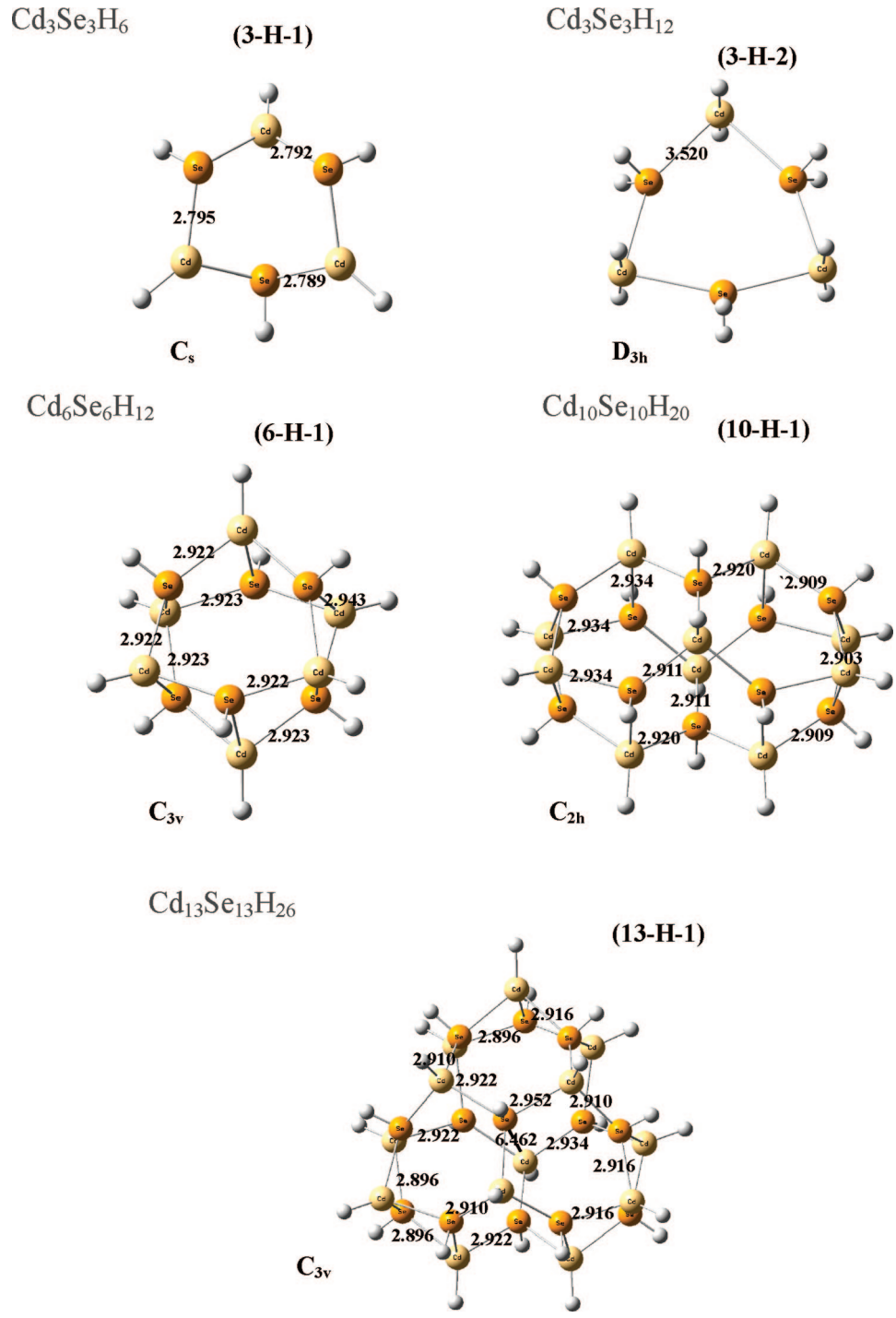

Figure 3. Geometry (bond lengths in Å) and point group of $Cd_nSe_nH_m$ (n = 3, 6, 10, 13).

of the valences in the Cd and Se atoms increases (from 2 in Cd_3Se_3 to 3 in Cd_6Se_6 and to 3 or 4 in $Cd_{10}Se_{10}$ and $Cd_{13}Se_{13}$). However, transitions to the third excited states show a peak at n = 3 (2.87 eV), then an increase from n = 6 to n = 13 (2.63, 2.72, 2.71 eV), exhibiting a somewhat irregular pattern.

The vertical transition energies of the Cys-bound Cd_nSe_n complexes, also listed in Table 1, are slightly blue-shifted by up to 0.18 eV from those of the bare CdSe clusters. As expected, the blue shift becomes smaller with increasing size of the CdSe cluster. Although the magnitudes of the calculated shifts for the CdSe−Cys complexes seem to be small, larger biomolecules such as polypeptides including many Cys are expected to give stronger blue shifts of the electronic spectra, assuming the same mode of coordination via carbonyl oxygen atoms. Thus, our predictions for the prototypical system will help to assign the experimental electronic spectra of the CdSe−Cys complexes.

III-5. The Effects of Hydrogen Passivation on Structure and Electronic Excitation on Nanocluster Core. We use hydrogen atoms to simulate ligands such as surface coordinating solvent molecules and stabilizing agents. Figure 3 presents the calculated structures and relative energies and Gibbs free energies at 298 K of the CdSe clusters passivated with the hydrogen atoms: $(CdSe)_nH_{2n}$−Cys (n = 3, 6, 10, 13). We find that for the nanocluster to be structurally stable each of the Cd (Se) atoms tend to be tetravalent and that full passivation of Cd_nSe_n (n = 6, 10, 13) by hydrogen atoms requires 2n numbers of hydrogen atoms. The only exception is $Cd_3Se_3H_{12}$, which requires 12 hydrogen atoms to satisfy tetravalent tendency of

TABLE 2: Electronic Energy *E* (Hartree), Zero Point Energy ZPE (kcal/mol), Vertical Electronic Excitation Energy VE (eV), and Oscillator Strength *f* to the Four Lowest Excited States of $Cd_nSe_nH_m$ and $Cd_nSe_nH_m$−Cys (n = 3, 6, 10, 13) Clusters

	E	ZPE	VE	*f*	symmetry
$Cd_3Se_3H_6$					
(3-H-1)	−175.557845	24.9	4.55, 4.65, 4.82, 4.91	0.0888, 0.0576, 0.0389, 0.0559	$^1A'\leftarrow X\ ^1A''$
$Cd_3Se_3H_{12}$					
(3-H-2)	−178.945649	48.0	5.08, 5.08, 5.08, 5.19	0.0000, 0.0000, 0.0038, 0.0000	$^1A_1\leftarrow X\ ^1B_1$
$Cd_3Se_3H_{12}$−Cys					
(3-H-c-1)	−901.029262	116.9	4.72, 5.01, 5.08, 5.09	0.0064, 0.0089, 0.0006, 0.0013	
(3-H-c-2)	−901.027227	117.2	5.03, 5.05, 5.16, 5.17	0.0008, 0.0014, 0.0039, 0.0009	
$Cd_6Se_6H_{12}$					
(6-H-1)	−351.153059	50.3	4.28, 4.28, 4.53, 4.53	0.0000, 0.0000, 0.1532, 0.1531	$^1A_1\leftarrow X\ ^1E$
$Cd_6Se_6H_{12}$−Cys					
(6-H-c-1)	−1073.24120	118.9	4.23, 4.44, 4.49, 4.52	0.1224, 0.0822, 0.0020, 0.0384	
(6-H-c-2)	−1073.24035	118.9	4.26, 4.47, 4.50, 4.55	0.1283, 0.0788, 0.0046, 0.0439	
(6-H-c-3)	−1073.23678	118.9	4.22, 4.32, 4.43, 4.53	0.0059, 0.0023, 0.0873, 0.0771	
$Cd_{10}Se_{10}H_{20}$					
(10-H-1)	−585.570566	84.3	4.26, 4.35, 4.36, 4.36	0.0000, 0.0000, 0.1262, 0.0000	$^1A_g\leftarrow X\ ^1B_u$
$Cd_{10}Se_{10}H_{20}$−Cys					
(10-H-c-1)	−1307.35978	153.4	4.11, 4.20, 4.37, 4.40	0.1303, 0.0393, 0.0237, 0.0635	
(10-H-c-2)	−1307.35682	153.3	4.21, 4.29, 4.32, 4.37	0.0041, 0.0842, 0.0284, 0.0113	
(10-H-c-3)	−1307.35545	153.2	4.19, 4.29, 4.32, 4.37	0.0325, 0.0447, 0.0436, 0.0791	
$Cd_{13}Se_{13}H_{26}$					
(13-H-1)	−760.851177	110.2	4.23, 4.24, 4.24, 4.27	0.0000, 0.0486, 0.0504, 0.1129	$^1A_1\leftarrow X\ ^1A_1$
$Cd_{13}Se_{13}H_{26}$−Cys					
(13-H-c-1)	−1482.93958	179.0	4.05, 4.12, 4.27, 4.27	0.0959, 0.0337, 0.0118, 0.0773	
(13-H-c-2)	−1482.93642	178.9	4.11, 4.22, 4.25, 4.28	0.0444, 0.0500, 0.0817, 0.1153	
(13-H-c-3)	−1482.93319	179.0	4.17, 4.24, 4.26, 4.28	0.0659, 0.0229, 0.0254, 0.0062	
$Cd_{13}Se_{13}H_{25}$ - Cys					
(13-H-b-1)	−1481.78774	170.3	3.51, 3.95, 4.02, 4.15	0.0189, 0.0743, 0.0231, 0.1034	
(13-H-b-2)	−1481.77579	167.7	3.54, 3.82, 4.10, 4.19	0.0044, 0.0005, 0.0024, 0.0088	
$Cd_{13}Se_{13}H_{24}$−Cys					
(13-H-t-b)	−1480.61442	159.1	2.95, 3.46, 3.58, 3.65	0.0070, 0.0026, 0.0900, 0.0006	
$Cd_{13}Se_{13}H_{25}$−Cys− Cys					
(13-H-b-b-1)	−2126.25462	212.5	3.14, 3.77, 3.88, 3.91	0.0154, 0.0022, 0.0088, 0.0830	
(13-H-b-b-2)	−2126.24969	214.3	3.28, 3.32, 3.85, 3.86	0.0144, 0.0139, 0.0688, 0.0143	
$Cd_{13}Se_{13}H_{24}$ - Cys- Cys					
(13-H-b-b-b)	−2125.08661	203.6	2.89, 2.98, 3.40, 3.58	0.0067, 0.0051, 0.0018, 0.0015	

the Cd (Se) atoms. The partially passivated cluster, $Cd_3Se_3H_6$, exhibits properties that are somewhat different from those of the fully passivated cluster $Cd_3Se_3H_{12}$, as discussed below.

Hydrogen passivation appears to weaken the Cd−Se bonds when the cluster size is small. The Cd−Se bond length (3.520 Å) in $Cd_3Se_3H_{12}$ is much larger than that (2.597 Å) in Cd_3Se_3. A large cluster appears to be structurally more "inert", as larger fully passivated clusters ($Cd_nSe_nH_{2n}$) are similar to their bare counterparts (Cd_nSe_n).

III-6. Hydrogen Passivation Blue Shifts the Electronic Excitations of Nanoclusters. The electronic excitation energies of $Cd_nSe_nH_{2n}$ and $Cd_nSe_nH_{2n}$−Cys to the four lowest excited states are listed in Table 2 along with the oscillator strengths. The transition energies (>4 eV) are much larger than those (<3 eV) of the bare Cd_nSe_n clusters.

For the smallest nanocluster (n = 3), we note that complete saturation of hydrogen atoms blue shifts the excitation energies to the lowest excited states from 5.0∼5.2 eV (for $Cd_3Se_3H_{12}$) from 4.6∼4.9 eV (for $Cd_3Se_3H_6$) and from 2.4∼3.3 eV (for Cd_3Se_3). We observe similarly increased excitation energies with hydrogen passivation for other cases of $Cd_nSe_nH_{2n}$ in contrast with Cd_nSe_n clusters. The excitation energy is sensitive to the effects of passivation due to the $\pi-\pi^*$ ($\sigma-\sigma^*$) character of the transitions in the bare (passivated) CdSe clusters, as we demonstrated previously for the silicon clusters.[61]

III-7. Cys-Binding Red Shifts the Electronic Excitations of Hydrogen-Passivated Nanoclusters. The calculated structures of the $Cd_nSe_nH_{2n}$−Cys complexes are given in Figure 4, and we find that in these lowest energy structures the carbonyl oxygen atom and the −SH group bridge the two nearest Cd atoms. Cys binding of the nanocluster appears to have opposite effects on transition energies in the presence of hydrogen passivation. We find that the transition energies red shift as the result of interactions between $Cd_nSe_nH_{2n}$ and Cys, in contrast with the blue shift induced by Cys in Cd_nSe_n clusters. The degree of the shifts in the electronic spectra is again small, decreasing from ∼0.3 eV for the lowest excitation in $Cd_3Se_3H_{12}$ to ∼0.1 eV for $Cd_{13}Se_{13}H_{26}$. The electronic excitation energies of the $Cd_nSe_nH_{2n}$ and $Cd_nSe_nH_{2n}$−Cys system are calculated to decrease smoothly as a function of the size (n).

III-8. Cd−S Bonding Increases the Red Shift Due to Cys- and Cys−Cys- Binding. One important issue concerning the CdSe−Cys system is the nature of interactions between CdSe and Cys in the complex. To our knowledge, the structural features of the CdSe−Cys system has not been elucidated unambiguously. For example, it has not been known which atomic pairs constitute the bridges between the CdSe core and the biomolecule. The fully passivated $Cd_nSe_nH_{2n}$ clusters may interact with Cys by forming the O−Cd−Cd−H type bonding arrangement as described in Figure 4, or $Cd_nSe_nH_{2n}$ and Cys may form other types of bonding by losing some hydrogen atoms of the acidic functional groups such as −COOH and −SH. Specifically, we wanted to know in what situation the sulfur atom in Cys may form a chemical bond with the Cd atom, as usually presumed.

The possibility of Cd−S bond formation is a reasonable hypothesis given the large bond enthalpy (49.8 kcal/mol). We allow possible formation of Cd−S bond by removing the two

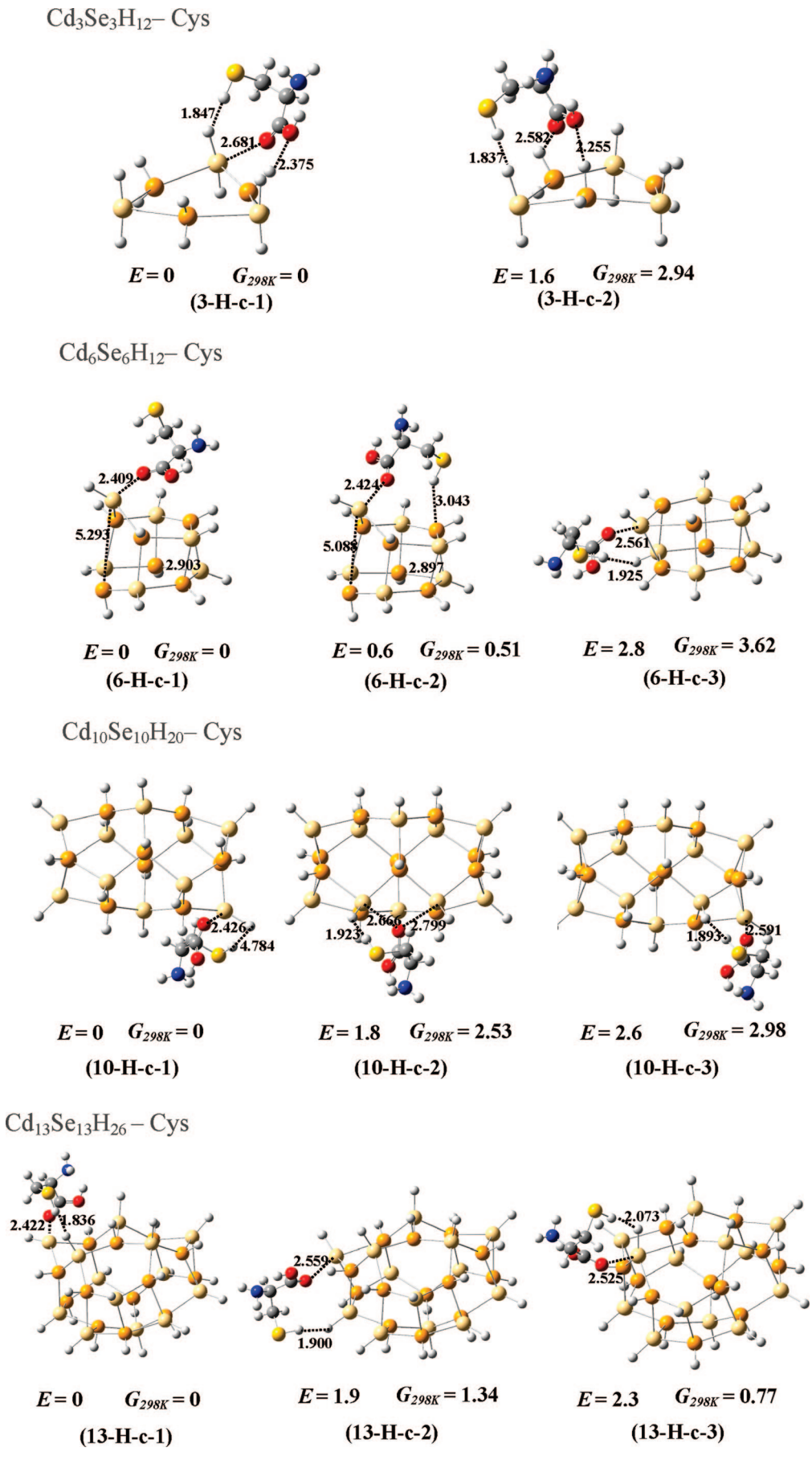

Figure 4. Geometry (bond lengths in Å), relative energy (kcal/mol), and relative Gibbs free energy (kcal/mol, at 298 K) of $Cd_nSe_nH_m$−Cys (n = 3, 6, 10, 13).

$Cd_{13}Se_{13}H_{25}$− Cys

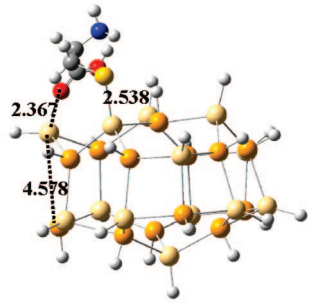

E = 0 G_{298K} = 0

(13-H-b-1)

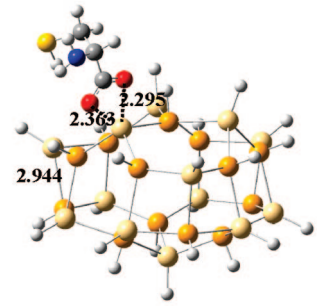

E = 4.9 G_{298K} = 0.76

(13-H-b-2)

$Cd_{13}Se_{13}H_{24}$− Cys

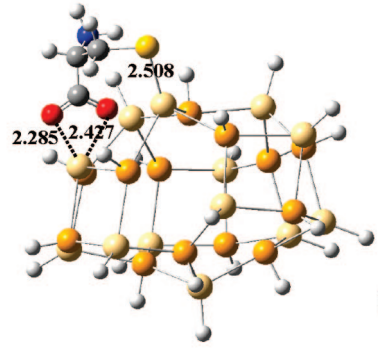

(13-H-t-b)

$Cd_{13}Se_{13}H_{24}$− Cys_Cys

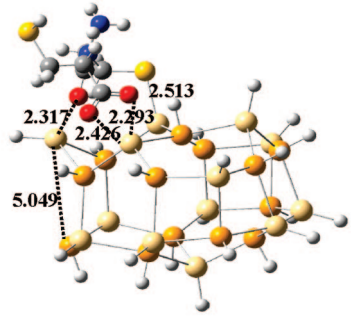

E = 0 G_{298K} = 0

(13-H-b-b-1)

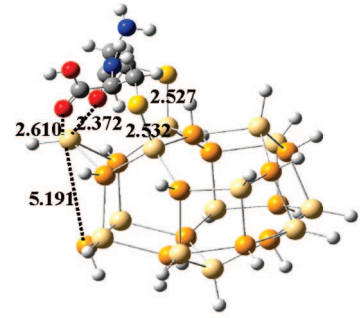

E = 4.9 G_{298K} = 6.49

(13-H-b-b-2)

$Cd_{13}Se_{13}H_{23}$− Cys_Cys

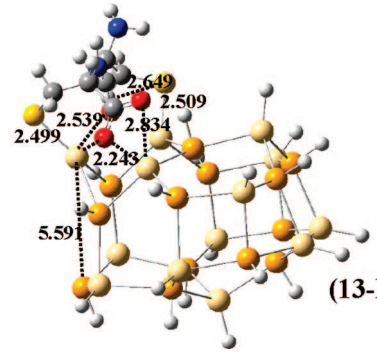

(13-H-b-b-b)

Figure 5. Geometry (bond lengths in Å), relative energy (kcal/mol), and relative Gibbs free energy (kcal/mol, at 298 K) of $Cd_{13}Se_{13}H_{25}$−Cys, $Cd_{13}Se_{13}H_{24}$−Cys $Cd_{13}Se_{13}H_{24}$−Cys−Cys, and $Cd_{13}Se_{13}H_{23}$−Cys−Cys.

hydrogen atoms from $Cd_{13}Se_{13}H_{26}$ and Cys and relax the entire bioconjugated nanocluster. If the equilibrium structure shows Cd−S bond formation, then it constitutes evidence of its likelihood. Figure 5 depicts the two complexes thus obtained. In the complex (13-H-b-1), the carbonyl oxygen binds to a Cd atom, whereas the S atom loses a hydrogen atom and forms a bond with the neighboring Cd. This isomer is much lower in energy (by ∼5 kcal/mol) than (13-H-b-2), in which the two oxygen atoms in the $-CO_2$ group bridge a Cd atom. This suggests that Cd−S bond formation is favored to a certain extent. We also find the equilibrium structure (13-H-t-b) in which Cys is bound to CdSe nanocluster by forming both Cd−S and Cd−OOC bonds with two hydrogen atoms of Cys and CdSe lost, respectively. Therefore, it seems that the O−Cd−Cd−S type four-centered bonding may be a prominent feature in the CdSe−Cys system.

This type of bonding exerts interesting effects on the electronic transition energies of these complexes, producing a significant red shift from the hydrogen-passivated clusters ($Cd_{13}Se_{13}H_{26}$). Table 2 shows that the shifts amount to ∼0.7 eV in (13-H-b-1) and ∼1.2 eV in (13-H-t-b), which seem to be quite large for interactions with a small biomolecule such as Cys. This correlation between the shift of excitation energies and the structure may be useful to distinguish between the bonding modes of Cys to the inorganic core.

To estimate the structure and the degree of influence of a polypeptide on the electronic spectra of the $Cd_{13}Se_{13}H_{26}$ system, we carried out similar analysis for the $Cd_{13}Se_{13}H_{24}$−Cys−Cys system. We find two structures of low energy, (13-H-b-b-1) and (13-H-b-b-2), in which the bonds are formed by losing four hydrogen atoms from Cys−Cys, Figure 5. In the lowest energy conformer (13-H-b-b-1), two carboxylic oxygen atoms bridge a Cd atom, while the sulfur and the oxygen atom in the amide group bind to neighboring Cd atoms. On the other hand, in (13-H-b-b-2) with energy higher by ∼5 kcal/mol, two sulfur atoms bond with neighboring Cd atoms, while the amide oxygen and carbonyl oxygen atom of the C-terminus bridge a Cd atom. We also obtain the structure (13-H-b-b-b) in which three bonds are formed between the passivated $Cd_{13}Se_{13}$ cluster and Cys−Cys (six hydrogen atoms lost), Cd−S, Cd−O, and Cd−OOC. In this context, we may deduce that in the lowest energy conformer of CdSe−polypeptide complex the carboxylic oxygen atoms of the C-terminus bind to a Cd atom, while the amide oxygen and sulfur atoms in the Cys residues interact with neighboring Cd atoms.

The Cys−Cys dipeptide seems to cause larger red shift of the excitation spectra (up to ∼1.4 eV), indicating that conjugation with a longer polypeptide may give rise to more significant changes in the electronic spectra of CdSe.

In conclusion, we calculated structures and electronic spectra for Cd_nSe_n−Cys and the $Cd_nSe_nH_{2n}$−Cys ($n \leq 13$). Interactions with Cys blue shift the electronic excitations of the bare CdSe. However, hydrogen passivation together with Cys-bind is found to red shift. We discover that a structural feature of the Cys-bound hydrogen-passivated nanocluster ($Cd_nSe_nH_{2n}$−Cys and −Cys−Cys system) is the four-membered ring O−Cd−H−Cd. We also showed that Cd−S (or both Cd−S and Cd−OOC) bonds are favorable when Cys (or Cys−Cys) forms covalent bonds with the hydrogen-passivated cluster. Thus, the CdSe−peptide including Cys seems to be characterized by O−Cd−S−Cd bonding pattern. This may be readily observed in excitation spectra, as shifts in the electronic spectra resulting from this type of bonding are predicted to be considerable (0.7∼1.4 eV). Experiments on this interesting system will be highly desirable.

Acknowledgment. This work was supported by the GRRC Grant, KISTI supercomputing center (KSC-2007-S00−1028), and by the Petroleum Research Fund.

Supporting Information Available: This material is available free of charge via the Internet at http://pubs.acs.org.

References and Notes

(1) Sarikaya, M.; Tamerler, C.; Jen, A.; Schulten, K.; Baneyx, F. *Nat. Mater.* **2004**, *2*, 577.
(2) Whaley, S.; English, D.; Hu, E.; Barbara, P.; Belcher, A. *Nature* **2000**, *405*, 665.
(3) Flynn, C.; Lee, S.-W.; Peelle, B.; Belcher, A. *Acta Mater.* **2003**, *51*, 5867.
(4) Seeman, N.; Belcher, A. *Proc. Natl. Acad. Sci. U.S.A.* **2002**, *99*, 6451.
(5) Peelle, B.; Krauland, E.; Wittrup, K.; Belcher, A. *Langmuir* **2005**, *21*, 6929.
(6) Pinaud, F.; Michalet, X.; Bentolila, L.; Tsay, J.; Doose, S.; Li, J.; Iyer, G.; Weiss, S. *Biomaterials* **2006**, *27*, 1679.
(7) Pinaud, F.; King, D.; Moore, H.-P.; Weiss, S. *J. Am. Chem. Soc.* **2004**, *126*, 6115.
(8) Smith, A.; Ruan, G.; Rhyner, M.; Nie, S. *Biomed. Eng.* **2006**, *34*, 3.
(9) Tsay, J.; Doose, S.; Weiss, S. *J. Am. Chem. Soc.* **2006**, *128*, 1639.
(10) Michalet, X.; Pinaud, F.; Bentolila, L.; Tsay, J.; Doose, S.; Li, J.; Sundaresan, G.; Wu, A.; Gambhir, S.; Weiss, S. *Science* **2005**, *307*, 538.
(11) Eichkorn, K.; Ahlrichs, R. *Chem. Phys. Lett.* **1998**, *288*, 235.
(12) Deglmann, P.; Ahlrichs, R.; Tsereteli, K. *J. Chem. Phys.* **2002**, *116*, 1585.
(13) Leung, K.; Whaley, K. B. *J. Chem. Phys.* **1999**, *110*, 11012.
(14) Troparevsky, M. C.; Chelikowsky, J. R. *J. Chem. Phys.* **2001**, *114*, 943.
(15) Troparevsky, M. C.; Kronik, L.; Chelikowsky, J. R. *J. Chem. Phys.* **2003**, *119*, 2284.
(16) Puzder, A.; Williamson, A. J.; Gygi, F.; Galli, G. *Phys. Rev. Lett.* **2004**, *92*, 217401.
(17) Peng, Z. A.; Peng, X. *J. Am. Chem. Soc.* **2001**, *123*, 1389.
(18) Nirmal, M.; Norris, D. J.; Kuno, M.; Bawendi, M. G.; Efros, A. L.; Rosen, M. *Phys. Rev. Lett.* **1995**, *75*, 3728.
(19) Efros, A. L.; Rosen, M.; Kuno, M.; Nirmal, M.; Norris, D. J.; Bawendi, M. G. *Phys. Rev. B* **1996**, *54*, 4843.
(20) Fisher, B. R.; Eisler, H. J.; Stott, N. E.; Bawendi, M. G. *J. Phys. Chem. B* **2004**, *108*, 143.
(21) Qu, L.; Peng, X. *J. Am. Chem. Soc.* **2002**, *124*, 2049.
(22) Ebenstein, Y.; Mokari, T.; Banin, U. *Appl. Phys. Lett.* **2002**, *80*, 4033.
(23) de Mello Donega, C.; Hickey, S. G.; Wuister, S. F.; Vanmaekelberg, D.; Meijerink, A. *J. Phys. Chem. B* **2003**, *107*, 489.
(24) Thoma, S. G.; Sanchez, A.; Provencio, P. P.; Abrams, B. L.; Wilcoxon, J. P. *J. Am. Chem. Soc.* **2005**, *127*, 7611.
(25) Joo, J.; Son, J. S.; Kwon, S. G.; Yu, J. H.; Hyeon, T. *J. Am. Chem. Soc.* **2006**, *128*, 5632.
(26) Jose, R.; Zhanpeisov, N. U.; Fukumura, H.; Baba, Y.; Ishikawa, M. *J. Am. Chem. Soc.* **2006**, *128*, 629.
(27) Jacobsohn, M.; Banin, U. *J. Phys. Chem. B* **1999**, *104*, 1.
(28) Li, L.-s.; Hu, J.; Yang, W.; Alivisatos, A. P *Nano Lett.* **2001**, *1*, 349.
(29) Zlateva, G.; Zhelev, Z.; Bakalova, R.; Kanno, I. *Inorg. Chem.* **2007**, *46*, 6212.
(30) Manna, L.; Scher, E. C.; Alivisatos, A. P. *J. Am. Chem. Soc.* **2000**, *122*, 12700.
(31) Jasieniak, J.; Mulvaney, P. *J. Am. Chem. Soc.* **2007**, *129*, 2841.
(32) Mattoussi, H.; Mauro, J. M.; Goldman, E. R.; Anderson, G. P.; Sundar, V. C.; Mikulec, F. V.; Bawendi, M. G. *J. Am. Chem. Soc.* **2000**, *122*, 12142.
(33) Tsay, J. M.; Doose, S.; Weiss, S. *J. Am. Chem. Soc.* **2006**, *128*, 1639.
(34) Gill, R.; Willner, I.; Shweky, I.; Banin, U. *J. Phys. Chem. B,* **2005**, *109*, 23715.
(35) Delehanty, J. B.; Medintz, I. L.; Pons, T.; Brunel, F. M.; Dawson, P. E.; Mattoussi, H. *Bioconjugate Chem.* **2006**, *17*, 920.
(36) Cohen, R.; Kronik, L.; Shanzer, A.; Cahen, D.; Liu, A.; Rosenwaks, Y.; Lorenz, J. K.; Ellis, A. B. *J. Am. Chem. Soc.* **1999**, *121*, 10545.
(37) Artemyev, M.; Kisiel, D.; Abmiotko, S.; Antipina, M. N.; Khomutov, G. B.; Kislov, V. V.; Rakhnyanskaya, A. A. *J. Am. Chem. Soc.* **2004**, *126*, 10594.
(38) Pinaud, F.; King, D.; Moore, H.-P.; Weiss, S. *J. Am. Chem. Soc.* **2004**, *126*, 6115.
(39) Chen, F.; Gerion, D *Nano Lett.,* **2004**, *4*, 1827,

(40) Patolsky, F.; Gill, R.; Weizmann, Y.; Mokari, T.; Banin, U.; Willner, I. *J. Am. Chem. Soc.* **2003**, *125*, 13918.
(41) Clapp, A. R.; Medintz, I. L.; Mauro, J. T.; Fisher, B. R.; Moungi, G.; Bawendi, M. G.; Mattoussi, H. *J. Am. Chem. Soc.* **2004**, *126*, 301.
(42) Aryal, B. P.; Benson, D. E. *J. Am. Chem. Soc.* **2006**, *128*, 15986.
(43) Sandros, M. G.; Gao, D.; Benson, D. E. *J. Am. Chem. Soc.* **2005**, *127*, 12198.
(44) Clapp, A. R.; Medintz, I. L.; Fisher, B. R.; Anderson, G. P.; Mattoussi, H. *J. Am. Chem. Soc.* **2005**, *127*, 1242.
(45) Bakalova, R.; Ohba, H.; Zhelev, Z.; Nagase, T.; Jose, R.; Ishikawa, M.; Baba, Y. *Nano Lett.* **2004**, *4*, 1567.
(46) Schlamp, M. C.; Peng, X.; Alivisatos, A. P. *J. Appl. Phys.* **1997**, *82*, 5837.
(47) Klimov, V. I.; Mikhailovsky, A. A.; Xu, S.; Malko, A.; Hollingsworth, J. A.; Leatherdale, C. A.; Eisler, H.-J.; Bawendi, M. G. *Science* **2000**, *290*, 314.
(48) Zhelev, Z.; Bakalova, R.; Ohba, H.; Jose, R.; Imai, Y.; Baba, Y. *Anal. Chem.* **2006**, *78*, 321.
(49) Behrens, S.; Bettenhausen, M.; Eichhöfer, A.; Fenske, D. *Angew. Chem., Int. Ed. Engl.* **1997**, *36*, 2797.
(50) Soloviev, V. N.; Eichhöfer, A.; Fenske, D.; Banin, U. *J. Am. Chem. Soc.* **2001**, *123*, 2354.
(51) Frisch, M. J.; Trucks, G. W.; Schlegel, H. B.; Scuseria, G. E.; Robb, M. A.; Cheeseman, J. R.; Montgomery, Jr., J. A.; Vreven, T.; Kudin, K. N. ; Burant, J. C.; Millam, J. M.; Iyengar, S. S.; Tomasi, J.; Barone, V.; Mennucci, B.; Cossi, M.; Scalmani, G.; Rega, N.; Petersson, G. A.; Nakatsuji, H.; Hada, M.; Ehara, M.; Toyota, K.; Fukuda, R.; Hasegawa, J.; Ishida, M.; Nakajima, T.; Honda, Y.; Kitao, O.; Nakai, H.; Klene, M.; Li, X.; Knox, J. E.; Hratchian, H. P.; Cross, J. B.; Bakken, V.; Adamo, C.; Jaramillo, J.; Gomperts, R.; Stratmann, R. E.; Yazyev, O. ; Austin, A. J.; Cammi,R.; Pomelli, C.; Ochterski, J. W.; Ayala, P. Y. ; Morokuma, K.; Voth, G. A.; Salvador, P.; Dannenberg, J. J. ; Zakrzewski, V. G.; Dapprich, S.; Daniels, A. D.; Strain, M. C.; Farkas, O.; Malick, D. K.; Rabuck, A. D.; Raghavachari, K.; Foresman, J. B.; Ortiz, J. V.; Cui, Q.; Baboul, A. G. ; Clifford, S.; Cioslowski, J.; Stefanov, B. B.; Liu, G.; Liashenko, A.; Piskorz, P. ; Komaromi, I.; Martin, R. L.; Fox, D. J.; Keith, T. ; Al-Laham, M. A.; Peng, C. Y.; Nanayakkara, A.; Challacombe, M.; Gill, P. M. W.; Johnson, B.; Chen, W.; Wong, M. W.; Gonzalez, C.; Pople, J. A. *Gaussian 03*; Gaussian, Inc.: Wallingford CT, 2004.
(52) Becke, A. D. *J. Chem. Phys.* **1993**, *98*, 5648.
(53) Lee, C.; Yang, W.; Parr, R. P. *Phys. Rev. B* **1988**, *37*, 785.
(54) Rempel, J.; Trout, B.; Bawendi, M.; Jensen, K. *J. Phys. Chem. B* **2006**, *110*, 18007.
(55) Pokrant, S.; Whaley, K. *Eur. Phys. J. D* **1999**, *6*, 255.
(56) Puzder, A.; Williamson, A.; Zaitseva, N.; Galli, G.; Manna, L.; Alivisatos, P. *Nano Lett.* **2004**, *4*, 2361.
(57) Cotton, F.; Barnes, R.; Bannister, E. *J. Chem. Soc.* **1960**, 2199.
(58) Burford, N.; Royan, B.; Spence, R.; Cameron, S.; Linden, A.; Rogers, R. *J. Chem. Soc., Dalton Trans.* **1990**, 1521.
(59) Kopping, J. T.; Patten, T. E. *J. Am. Chem. Soc.* **2008**, *130*, 5689.
(60) Rabani, E. *J. Chem. Phys.* **2001**, *115*, 1493.
(61) Park, S.-W.; Lee, S.; Neuhauser, D. *J. Phys. Chem. A* **2006**, *110*, 7173.

JP8062299